

# Multi-analytical platform metabolomic approach to study miltefosine mechanism of action and resistance in *Leishmania*

Gisele A. B. Canuto · Emerson A. Castilho-Martins ·  
Marina F. M. Tavares · Luis Rivas · Coral Barbas ·  
Ángeles López-González

Received: 13 January 2014 / Revised: 3 March 2014 / Accepted: 17 March 2014 / Published online: 11 April 2014  
© Springer-Verlag Berlin Heidelberg 2014

**Abstract** Miltefosine (MT) (hexadecylphosphocholine) was implemented to cope with resistance against antimonials, the classical treatment in Leishmaniasis. Given the scarcity of anti- *Leishmania* (*L*) drugs and the increasing appearance of resistance, there is an obvious need for understanding the mechanism of action and development of such resistance. Metabolomics is an increasingly popular tool in the life sciences due to it being a relatively fast and accurate technique that can be applied either with a particular focus or in a global manner to reveal new knowledge about biological systems. Three analytical platforms, gas chromatography (GC), liquid chromatography (LC) and capillary electrophoresis (CE) have been coupled to mass spectrometry (MS) to obtain a broad picture of metabolic changes in the parasite. Impairment of the polyamine metabolism from arginine (Arg) to trypanothione in susceptible parasites treated with MT was in some way expected, considering the reactive oxygen species (ROS) production described for MT. Importantly, in resistant parasites an

increase in the levels of amino acids was the most outstanding feature, probably related to the adaptation of the resistant strain for its survival inside the parasitophorous vacuole.

**Keywords** Miltefosine · *Leishmania* (*L.*) *donovani* · Metabolic fingerprinting · Mass-spectrometry · Drug action · Resistance

## Introduction

The term leishmaniasis encompasses the different infections caused by protozoal species belonging to the genus *Leishmania*. Under clinical criteria, they are classified into three major groups: cutaneous leishmaniasis (CL), mucocutaneous leishmaniasis (MCL) and visceral leishmaniasis (VL), ranked in order of increasing severity, where the latter can be fatal if untreated [1]. According to a recent update [2], leishmaniasis is prevalent in 98 countries, mostly in tropical and subtropical areas, with an annual incidence of 0.2 to 0.4 million cases for VL and of 0.7 to 1.2 million for CL plus MCL.

Despite significant recent advances in *Leishmania* vaccines [3, 4], current solutions for this disease rely almost exclusively on chemotherapy, and until recently treatments have been based on antimonials drugs and still this is the case in countries with high population and weak economies [5–7]. Furthermore, its efficacy is increasingly eroded by progressive resistance, significant side-effects and high cost, a heavy burden for the majority of patients [8], who live under poverty standards.

Miltefosine (hexadecylphosphocholine), was developed as an antitumor drug, but also has shown to have activity against *Leishmania*. It has the advantage of being administered as an oral drug, readily dispensed in hospitals and used in North-west India as an alternative treatment to antimonial resistant

G. A. B. Canuto · E. A. Castilho-Martins · C. Barbas ·  
Á. López-González (✉)  
Centro de Metabolómica y Bioanálisis (CEMBIO), Unidad  
Metabolómica, Interacciones y Bioanálisis (UMIB), Facultad de  
Farmacia, Universidad CEU San Pablo, Campus Monteprincipe,  
Boadilla del Monte 28668, Madrid, Spain  
e-mail: alopgon@ceu.es

G. A. B. Canuto · M. F. M. Tavares  
Institute of Chemistry, University of São Paulo (USP),  
Campus São Paulo. São Paulo, 05508-000 São Paulo, Brazil

E. A. Castilho-Martins  
Collegiate of Medicine, Federal University of Amapá,  
68903-419 Macapá, Brazil

L. Rivas (✉)  
Centro de Investigaciones Biológicas (CSIC),  
Unidad Metabolómica, Interacciones y Bioanálisis (UMIB),  
Ramiro de Maeztu 9, 28040 Madrid, Spain  
e-mail: luis.rivas@cib.csic.es

CL and VL. Antimonial resistance is a rising problem and exists in almost 60 % of patients in this aforementioned area [9, 10]. Miltefosine achieved a 97 % cure rate on *L. (L.) donovani* infection [6], although more recent reports show a decrease in its efficacy [11–14].

The molecular basis of MT leishmanicidal activity has not yet been completely unveiled, in any case leading to the elimination of the parasite through an incidental cell death process [15]. Its molecular properties [16] along with its high intracellular concentration will favor a multitarget lethal mechanism [17]: inhibition of choline transport [18], disturbances in the biosynthesis of ether-lipids [19] and phospholipids with inversion of the phosphatidylcholine (PC)/phosphatidylethanolamine (PE) ratio [20–22] and mitochondrial dysfunction with the release of iron superoxide dismutase A into the cytoplasm [23] as well as inhibition of cytochrome c oxidase [24]. Concerning the latter, overexpression of the Cox9 subunit of cytochrome oxidase reverts miltefosine susceptibility and associated cell death [25], although its validation in *Leishmania* is still missing. Arguably, it is feasible that mitochondrial dysfunction leading to an enhanced production of ROS will play a leading role in the lethal mechanism of MT, triggered by an increase in mitochondrial ROS production. This notion has been supported by transcriptomics analysis of MT responsive and unresponsive *L. donovani* strains that have higher expression of genes involved in anti-oxidant mechanisms [26, 27] and by the reporting of cross-resistance to miltefosine with other drugs inducing ROS production, except paromomycin, that kills *Leishmania* through a ROS-independent mechanism [12].

Resistance against MT in *Leishmania* is easily induced *in vitro* by growth under increasing drug exposure [12, 28], with a faulty MT intracellular accumulation as the outcome [17, 29]. This occurs either by loss-of-function mutations [28, 30] or under expression [31] of any of the two components of its uptake system, due to an aminophospholipid translocase (a P-type ATPase) and its regulatory unit Ldros3 [30], or by drug efflux carried out by ABC transporters [32, 33]. Whole genome sequencing of *L. major* MT resistant strains has detected mutations in  $\alpha$ -adaptin and pyridoxal kinase, the latter being accompanied by additional mutations of the MT transporter [34]. In clinical settings, a single polymorphism in the aminophospholipase translocase gene has been reported in a *L. infantum* MT-resistant French isolate [35], but none of the mutations in any of the two subunits of the MT uptake system were detected in *L. (L.) donovani* isolates from Indian patients where MT treatment failed [36].

The scarcity of new leads in the pipeline for leishmaniasis imposes the importance of preservation of the current drugs. To this end, the use of combined therapy has been recommended by the World Health Organization [6], however, multidrug resistant parasites against them have been recently discovered *in vitro* [37]. The quest for judicious drug combination to prevent or avert resistance, or to potentiate MT action

on *Leishmania*, requires the definition of the overall changes caused by resistance or by MT treatment on this parasite.

In this sense, metabolomics provides the ultimate result of the biological target challenged by the drug or condition under study, through the identification and quantification of metabolites (< 1000 Da) present in biofluids, cells and tissues under a given condition [38]. Implementation of this technique has been fuelled in the last few years by the rapid advances in analytical methods of high-resolution nuclear magnetic resonance (NMR) spectroscopy [39, 40] and mass spectrometry (MS) [41] coupled to separation techniques such as capillary electrophoresis (CE) [42], liquid chromatography- (LC) [43], gas chromatography- (GC) [44] or hydrophilic interaction chromatography (HILIC) [45]. Obtaining a metabolomic fingerprint as complete as possible requires the combination of several separation techniques, inherent to the highly diverse chemical structure of metabolites.

For *Leishmania*, metabolomics is of the highest relevance among the “omics” strategies; the capacity of transcriptomics to provide an accurate snapshot of the physiology of the organism perturbed by a drug or specific situation, is partially blurred due to the extremely high post-transcriptional regulation of gene expression in trypanosomatids [46]. Proteomics partially overcomes this hurdle: it has been extensively employed to decipher mechanisms of drug resistance [47–49], but this still overlooks some metabolic subtleties that are inherent to the complexity of the intracellular environment. A metabolome database for *Leishmania* has been developed [50], and a number comprehensive reviews have been published [51–53]. Metabolomic studies have been carried out previously on *Leishmania* [51, 54, 55] including the study of drug activity and resistance [56, 57].

We have evaluated metabolic changes involved in the mechanism of action and resistance of MT in *Leishmania (L.) donovani*, using complementary analytical platforms coupled to MS, to obtain a comprehensive overview of the changes in the metabolic landscape underlying this drug. Our data provide insights into the alteration of polyamine pathway biosynthesis as well as changes in the amino acid pool and reinforces the suspected mechanism of action *via* incidental death process previously reported.

## Materials and methods

### Reagents

Methanol (LC-MS grade), heptane (GC-MS grade), chloroform (MS grade), acetonitrile (LC-MS grade), isopropanol (LC-MS grade), formic acid (MS grade), pyridine (silylation grade), C18:0 methyl ester and *O*-methoxyamine hydrochloride were purchased from Sigma-Aldrich (Taufkirchen, Germany); *N,O*-bis(trimethylsilyl) trifluoroacetamide (BSTFA)

plus 1 % trimethylchlorosilane (TMCS) was purchased from Pierce Chemical Co (Rockford, IL, USA) and references masses purine and HP-0921 (hexakis-(1H,1H,3H-tetrafluoropentoxo)-phosphazene) were from Agilent (atmospheric pressure inlet – time of flight (API-TOF) reference mass solution kit). Milli-Qplus 185 was provided by Millipore (Billerica, MA, USA),

#### *Leishmania* parasites culture

Promastigotes of the *Leishmania (L.) donovani* strain MHOM/ET/67/L82 and their MT resistant homologues were kindly provided by Prof. S. L. Croft (London School of Hygiene and Tropical Medicine). Miltefosine resistance in this strain was induced by growth of the parasites under step-wise increasing drug exposure, doubling the concentration once the growth rate of the resistant parasites matched that of the wild type [58]. Parasites were grown in Roswell Park Memorial Institute medium (RPMI-1640) supplemented with 10 % heat inactivated fetal calf serum at 26°C. Large scale culture was carried out in a roller Apparatus (Gibco, Cell Culture) with an inoculum of  $4 \times 10^5$  promastigotes/mL. Once they reached mid-exponential phase ( $8 \times 10^6$  promastigotes/mL) they were transferred into the same volume of fresh medium, and incubated with  $10 \mu\text{mol.L}^{-1}$  MT (a concentration causing 90 % mortality, measured after 12 h), named as susceptible treated (ST), or without the drug (named as susceptible non-treated (SNT)). *L. (L.) donovani* promastigotes resistant to MT (named as resistant (R40)) were grown as described above but with the addition of  $40 \mu\text{mol.L}^{-1}$  MT in the growth medium. Once harvested, parasites were washed twice with Hanks buffer chilled previously at 4°C, immediately frozen in liquid N<sub>2</sub>, and kept at – 80°C until analysis. Six replicates of each group of samples (ST, SNT and R40) were in themetabolomics studies by the three analytical techniques, except in the case of GC-MS where 5 replicates were analyzed from the R40 group.

#### GC-MS fingerprinting

For GC-MS analysis, pellets corresponding to  $4 \times 10^7$  *L. (L.) donovani* promastigotes were re-suspended and lysed by addition of 350  $\mu\text{L}$  methanol:water:chloroform 3:1:1 (v:v:v) at 4°C followed by shaking in a Tissuelyser LT (Qiagen, Germany) (2 glass balls, 2 mm, 20 min, 50 Hz). Subsequently, samples were centrifuged ( $15,700 \times g$ , 15 min, 4°C) in a 5415 R Eppendorf centrifuge. The supernatant was removed, and 200  $\mu\text{L}$  from each sample were used for derivatization. Additionally, 100  $\mu\text{L}$  aliquots of the supernatants from each sample were pooled and used to prepare the QCs (Quality Controls – obtained from the pool of the whole set of samples) by an identical procedure. A blank was also prepared following the

same extraction and derivatization procedures, and analyzed at the beginning and at the end of the sequence.

For analysis, 200  $\mu\text{L}$  of sample supernatant and QCs were evaporated to dryness in a SpeedVac operated at 30°C. Following this, 10  $\mu\text{L}$  of *O*-methoxyamine hydrochloride ( $15 \text{ mg.mL}^{-1}$ ) in pyridine were added to each GC vial and mixed vigorously with a vortex FB 15024 (Fisher Scientific, Spain). Samples were subsequently incubated in the dark at room temperature for 16 h to allow methoximation. For silylation, 10  $\mu\text{L}$  of BSTFA with 1 % TMCS (v/v) were added and vortexed for 5 min; before vials were placed into an oven for 1 h at 70°C. Finally, 100  $\mu\text{L}$  of  $10 \text{ mg.mL}^{-1}$  of C18:0 methyl ester in heptane (internal standard) were added and samples were vortexed and analyzed by GC-MS.

GC-MS instrumentation: 2.0  $\mu\text{L}$  of the derivatized samples were analyzed in an Agilent 7890A Gas Chromatograph coupled with a Quadrupole analyzer Mass Spectrometer (5975 inert MSD, Agilent) and an autosampler (7693, Agilent), controlled by ChemStation software (G1701EA E.02.00.493, Agilent). Helium was used as the carrier gas at a constant flow rate of  $1.0 \text{ mL.min}^{-1}$  through the column (30 m length, 0.25 mm i.d. (internal diameter)) with a chemically bonded DB5-MS film 95 % dimethyl/ 5 % diphenyl polysiloxane stationary phase (J&W Scientific, Folsom, CA). The injector temperature was 250°C and the split ratio was 1:10. The initial oven temperature of the column was 60°C; 1 min after injection the temperature was raised to 325°C through a  $10 \text{ }^\circ\text{C.min}^{-1}$  gradient and held for 10 min before cooling-down (37.5 min run time). The mass spectrometer was operated in full-scan mode from mass to charge ratio (*m/z*) 50 to 600 at a rate 2.0 spectra/s. The transfer line, filament source and quadrupole temperatures were 290, 230 and 150°C, respectively.

#### LC-MS fingerprinting

For LC-MS and CE-MS analysis: pellets corresponding to  $4 \times 10^7$  resuspended and lysed by addition of 350  $\mu\text{L}$  methanol/water 1/1 (v/v) at 4°C and further shaking in Tissuelyser LT (Qiagen, Germany) (2 glass balls 2 mm diameter, 20 min, 50 Hz). Subsequently, samples were centrifuged (centrifuge 5415 R, Eppendorf) at  $15,700 \times g$  for 15 min (4°C). The supernatant was split into two aliquots: 200  $\mu\text{L}$  to be used for direct injection in LC-MS and 100  $\mu\text{L}$  to be treated for further analysis in CE-MS.

The LC-MS instrumentation consisted of an Agilent 1200 Series HPLC with a degasser, two binary pumps and an autosampler, coupled to a QTOF (quadrupole time-of-flight) (6520, Agilent), controlled by Mass Hunter Workstation Data Acquisition (B.04.00, Agilent). The coupling was equipped with an electrospray ionization (ESI) source. 15  $\mu\text{L}$  of sample were injected onto a reverse-phase column at 40°C (Supelco

Discovery HS, C18, 150×2.1 mm i.d., 3.0 μm, Bellefonte, PA, USA) with a pre-column (Supelco Discovery HS, C18, 2.0 cm×2.1 mm i.d., 3.0 μm, Bellefonte, PA, USA). The system was operated a flow rate of 0.6 mL.min<sup>-1</sup> using a mobile phase composed of: A – MilliQ water with 0.1 % (v/v) formic acid and B – acetonitrile with 0.1 % (v/v) formic acid. The gradient was 25 to 95 % B in 40 min, and returned to starting conditions after 1 min afterwards, the column was re-equilibrated under these conditions until 50 min. The QTOF system was operated in positive Dual Electrospray Ionization mode in full scan from *m/z* 100 to 1000 at a rate 1.02 scan/s. Electrospray conditions were: capillary voltage 3000 V; drying gas at 330°C and flow rate of 10.5 L.min<sup>-1</sup>; nebulizer pressure 52 psi; fragmentor 175 V; octopole 750 V; skimmer 65 V. During the analysis two reference masses were used: 121.0509 – purine (C<sub>5</sub>H<sub>4</sub>N<sub>4</sub>) and 922.0098 – HP-0921 (C<sub>18</sub>H<sub>18</sub>O<sub>6</sub>N<sub>3</sub>P<sub>3</sub>F<sub>24</sub>), to allow constant mass correction.

### CE-MS

Parasite extraction is carried out as for LC-MS. 100 μL of supernatant was transferred into a new tube and evaporated to dryness using a SpeedVac at 35°C. The metabolite extracts were resuspended in 100 μL MilliQ water, centrifuged at 15,700 × *g* for 15 min (4°C) and supernatants analyzed by CE-MS.

The system used was a Capillary Electrophoresis (7100 Agilent) coupled to a TOF Mass Spectrometer (6224 Agilent). The CE mode was controlled by ChemStation software (B.04.03, Agilent) and MS mode by MassHunter Workstation Data Analysis (B.02.01, Agilent). The separation occurred in a fused-silica capillary (Agilent) (total length, 100 cm; 50 μm internal diameter). Separations were carried out in normal polarity with a background electrolyte containing 0.8 mol.L<sup>-1</sup> formic acid in 10 % methanol (v/v) at 20°C. New capillaries were pre-treated with a flush of: NaOH 1.0 mol.L<sup>-1</sup> for 30 min, followed by MilliQ water for 30 min and background electrolyte for 30 min. Before each analysis the capillary was conditioned by flushing the background electrolyte for 5 min (950 mbars pressure). The sheath liquid (4 μL.min<sup>-1</sup>) was methanol/water (1/1, v/v) containing 1.0 mmol.L<sup>-1</sup> formic acid with two reference masses: 121.0509 – purine (C<sub>5</sub>H<sub>4</sub>N<sub>4</sub>) and 922.0098 – HP-0921 (C<sub>18</sub>H<sub>18</sub>O<sub>6</sub>N<sub>3</sub>P<sub>3</sub>F<sub>24</sub>), to allow correction and high accurate mass in the MS. Samples were hydrodynamically injected at 50 mbar for 50 s. Stacking was carried out by applying the background electrolyte at 100 mbar for 10 s. The separation voltage was 30 kV with 25 mbar of internal pressure and the analyses were carried out in 30 min. The optimized MS parameters were: fragmentor 100 V, Skimmer 65 V, octopole 750 V, nebulizer pressure 20 psi, drying gas temperature at 200°C and flow rate 12.0 L.min<sup>-1</sup>. The capillary voltage was 3500 V. Data were

acquired in positive Dual-ESI mode with a full scan from *m/z* 80 to 1000 at a rate 1.02 scan/s.

### Quality Controls (QCs)

QCs samples were prepared by pooling equal volumes of each sample (all groups) and analyzed throughout the run. The same procedure was followed for the three techniques, however for GC-MS the QCs were prepared before the derivatization step. Six QCs were used in data treatment in each technique.

### Data Treatment and Statistical Analysis

The treatment of the data obtained by GC-MS analysis consisted of compound identification, using the Fiehn RTL Library (FiehnLib) and the National Institute of Standards and Technology mass spectra library (NIST MS, 2.0 g), in the ChemStation software PBM algorithm (G1701EA E.02.00.493, Agilent), with a correct assignment based on the coincidence of the retention time and the spectrum profile. The GC-MS data were normalized with respect to the internal standard (C18:0 methyl ester). Subsequently, deconvolution was performed using Automated Mass spectral Deconvolution and Identification System (AMDIS 2.69) software to identify co-eluting compounds followed by statistical analysis.

Background noise and unrelated ions were eliminated from LC-MS and CE-MS data by the Molecular Feature Extraction (MFE) tool in the Mass Hunter Qualitative Analysis Software B.04.00 (Agilent). The filtering and alignment of the data were performed with Mass Profiler Professional B.02.01 (Agilent) software by selection of features into the range 5.0 to 40.0 min (to LC-MS) and 6.0 to 22.0 min (CE-MS). Some significant compounds were confirmed by LC-MS/MS using a QTOF (model 6520, Agilent). Experiments were repeated with identical chromatographic conditions for samples and patterns, as described above. Ions were targeted for collision-induced dissociation (CID) fragmentation on the flight based on the previously determined accurate mass and retention time.

From the three analytical platforms selected, compounds with statistically significant differences were obtained by the comparisons: ST vs. SNT (treatment effect) and R40 vs. SNT (resistance effect). Features and compounds from GC-MS were filtered by selection of masses present in at least 75 % of the samples in one of two groups (ST vs. SNT or R40 vs. SNT). Differences among samples were evaluated by using Student's *t* test p-value < 0.05 (Microsoft excel) and multivariate analysis (Jack Knife from orthogonal projections to latent structures discriminant analysis models (OPLS-DA)) was performed by SIMCA-P+software (12.0.1 versions, Umetrics).

For LC-MS and CE-MS accurate masses of features with significant differences were searched against METLIN (<http://metlin.scripps.edu>) public database and MassTrix (<http://metabolomics.helmholtz-muenchen.de/masstrix2/>) [59].

## Results and discussion

As mentioned in the introduction, the mechanism of action of MT is not yet fully unveiled, but its small size, amphipathic nature and its high intracellular concentration [24], will favor a multi-targeted mechanism. MT is supposed to interact with cell membranes [60], and kill parasites via oxidative stress [24, 61]. As such, resistance relies on either avoidance of intracellular accumulation of the drug [30], or to prevention of induction of incidental cell death [12] as the final lethal process where the different detrimental effects of the drug converge. Lipidomics was, as expected, the first choice among the “omics” [21, 22, 62, 63], mainly because MT is an alkyllysophospholipid mimetic, that can easily integrate into membranes resulting in changes in membrane architecture [20]. Indeed, changes in phospholipid and sterol composition have been described for tumorous cells treated with MT [64].

MT resistance of the *Leishmania* strain used in this work was due to dysfunction of the transport system of MT [28]; because this aminophospholipid translocase also plays a physiological role to keep aminophospholipid asymmetry between

both sides of the membrane, resistance also affects the normal physiology of the parasite. However because resistant parasites maintain an adequate growth rate *in vitro* and virulence *in vivo* [65], retooling of the metabolism will be required to establish a check and balance homeostasis of the parasite. In this regard the new metabolomic techniques will be extremely useful.

Metabolites of *L. (L.) donovani* extracts were analyzed by GC-MS, LC-MS and CE-MS, in order to obtain a metabolic phenotype as extensive as possible as well as to assess the complementarity of these techniques.

The performance of these separation techniques was evaluated by building principal component analysis PCA models (Fig 1), using the SIMCAP+ software (12.0.1.0 versions, Umetrics), consisting of a multivariate analysis where the model is constructed by grouping different entities to optimize group clustering. For the current work the following groups were established: susceptible non-treated (SNT), susceptible treated (ST) and resistant (R40), while quality controls (QCs), obtained from the pool of the whole set of samples, were predicted. PCA models were constructed with the data matrix obtained with all detected features after only eliminating the background noise and performing alignment of all samples, including QCs. The location of the QCs in a well-defined area of the plot demonstrated first, that separation into these three groups is based on a real variability, and secondly that techniques and methods possess stability and reproducibility, as observed in Fig 1.

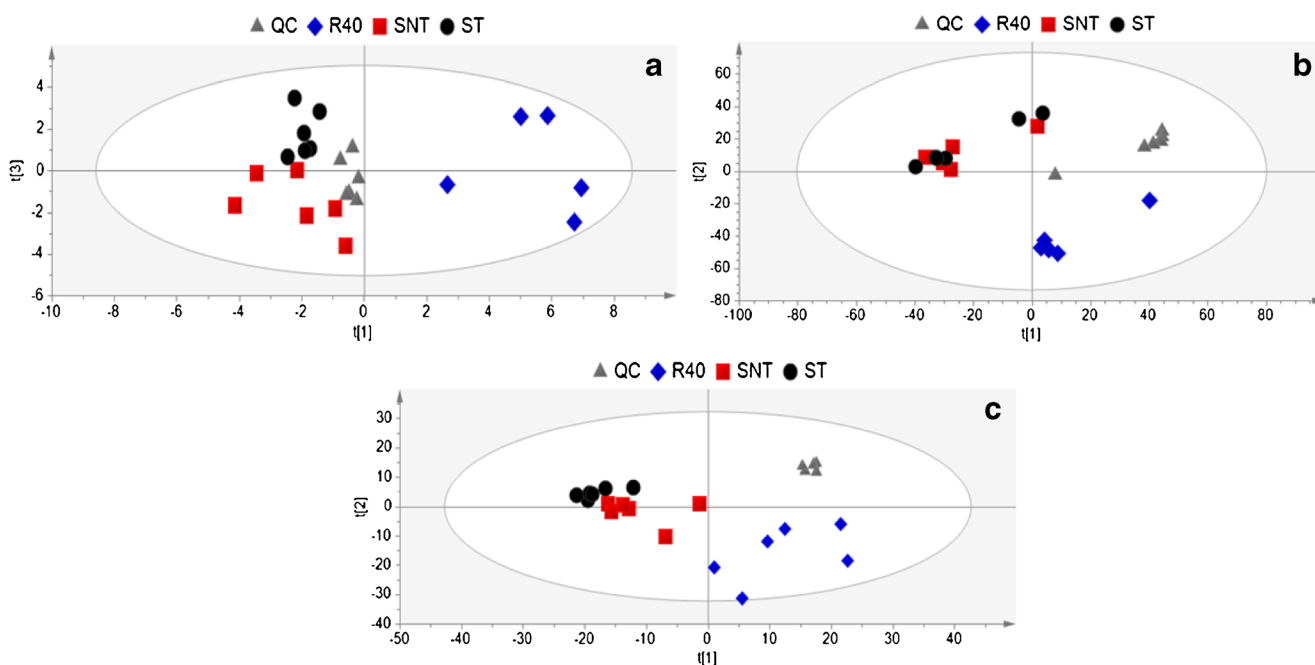


**Fig. 1** Scores plot for PCA models built with raw data set obtained with quality controls (QC) – gray triangle, susceptible non-treated (SNT) – red box, susceptible treated (ST) – black circle and miltefosine resistant (R40) – blue diamond, for *L. (L.) donovani*. **a)** Scores plot of GC-MS data (explained variance  $R^2=0.729$  and predicted variance  $Q^2=0.468$ ), **b)**

Scores plot LC-MS data (explained variance  $R^2=0.494$  and predicted variance  $Q^2=0.220$ ), and **c)** Scores plot CE-MS data (explained variance  $R^2=0.421$  and predicted variance  $Q^2=0.167$ ). Six replicates of each group of samples were analyzed, except in the case R40 by GC-MS

Once the methodology was considered appropriate, samples, without QCs, were realigned and filtered by a selection of masses present in at least 75 % of the samples in one of two groups (ST vs. SNT or R40 vs. SNT), using the software Mass Profiler Professional B.02.01 (Agilent). Score plots of partial least squares discriminant analysis (PLS-DA) were constructed and the prediction ability of the models was represented by  $Q^2$  values above 0.85. Clustering of the three groups of parasites is shown in Fig 2, by the use of the scores plot of two components. Statistical differences was obtained for 2 comparisons (ST vs. SNT and R40 vs. SNT) by multivariate analysis (OPLS-DA models and Jack Knife evaluation), Fig 3 shows OPLS-DA scores plot for study treatment effects and resistance effects, in the three analytical techniques. Obtained models were validated by cross-validation tools, using the leave 1/3 out approach. The data set was divided into three parts and 1/3 of the samples were excluded to build a model with the remaining 2/3 of samples. Excluded samples were then predicted by this new model and the procedure was repeated until all samples had been predicted at least once. Each time the percentage of correctly classified samples was calculated. Samples excluded were always perfectly predicted by the model (100 % samples classified correctly) in all cases. The models were validated by generating receiver operating characteristic (ROC) curves. Herein the Y-predicted for each sample in each model was plotted as a function of the true

positive (TPR) and false positive rates (FPR) with the real class. For all 6 models in the three analytical platforms, the sensitivity (TPR) and the specificity given by the area under the curve (AUC) was 100 %. Therefore the class prediction for the samples was 100 % classified correctly in all cases. After treatment of the data obtained from the three techniques employed (alignment, filtering and statistical analysis), final results are compiled in Table 1.

The number of compounds identified within metabolic pathways of the parasites with statistical significance was 16 for GC-MS (Table 2), while for LC-MS and CE-MS were of 24 and 48 masses respectively. Altogether, those compounds with a  $p$ -value < 0.05 for the respective changes in the treatment effect (ST vs. SNT) and resistance effect (R40 vs. SNT), are presented in Table 2. Some significant compounds identified by LC-MS were confirmed by MS/MS analysis and their fragmentation patterns appear in Table 2. After the identification step, several resulting significant masses were submitted to MassTrix (<http://metabolomics.helmholtz-muenchen.de/masstrix2/>) [59].

Different metabolic analyses in *Leishmania* have been previously reported using LC-MS or HILIC-MS [21, 57, 66]. In our case we used a combined analysis of GC-MS, LC-MS/MS and CE-MS. Since their respective separations rely on different physicochemical properties, the final outcome is complementary, providing a wider metabolic

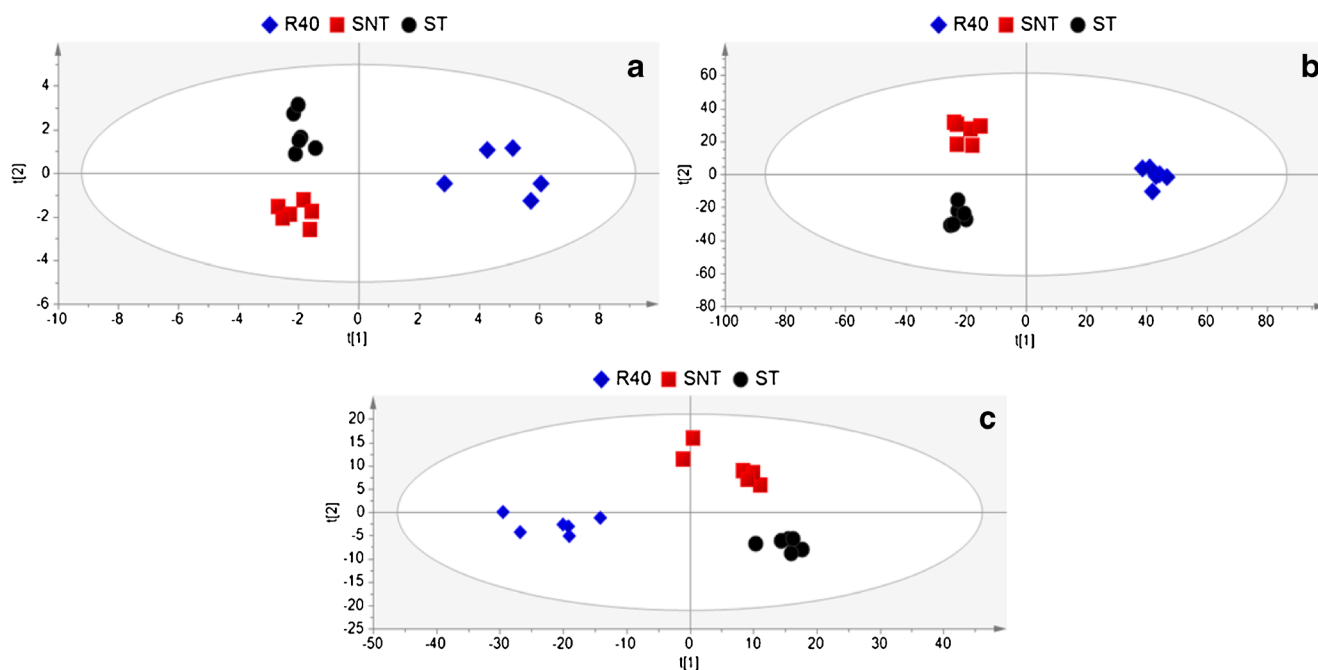


**Fig. 2** Scores plot for PLS-DA model built for three groups of samples, susceptible non-treated (SNT) – red box, susceptible treated (ST) – black circle and miltefosine resistant (R40) – blue diamond, of *L. (L.) donovani* (after alignment and filtering – presents in 75 % at least 1 of 2 comparisons). **a)** Scores plot of GC-MS normalized data (with internal standard C18:0 methyl ester), quality parameters of the model:  $R^2=0.947$

and  $Q^2=0.853$ , **b)** Scores plot of LC-MS analyzed data, quality parameters of the model:  $R^2=0.994$  and  $Q^2=0.929$ , and **c)** Scores plot of CE-MS analyzed data, quality parameters of the model:  $R^2=0.997$  and  $Q^2=0.893$ . Six replicates of each group of samples were analyzed, except in the case R40 by GC-MS

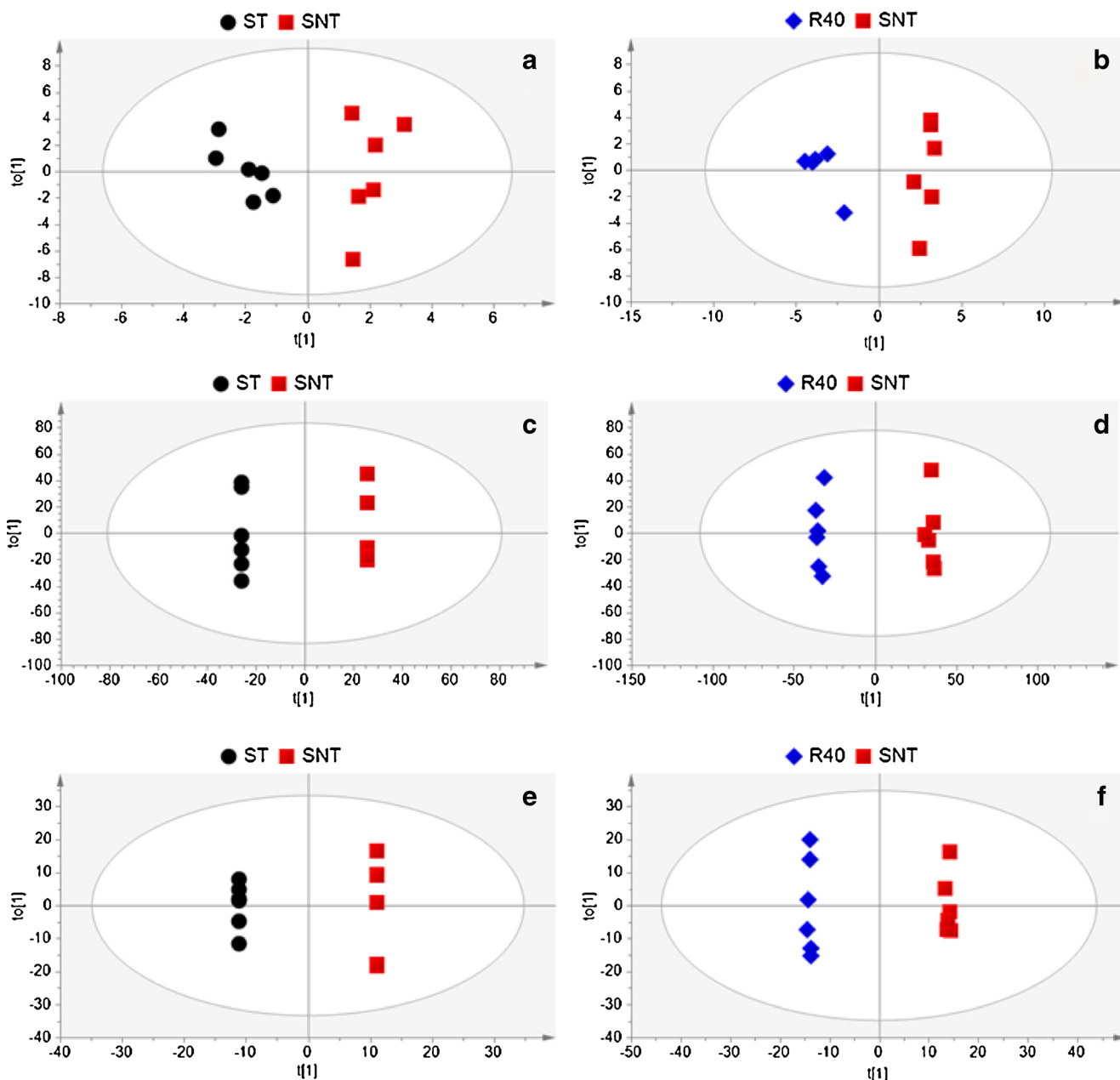


**Fig. 3** Scores plot for OPLS-DA model built for two comparisons (treatment – ST vs. SNT and resistance – R40 vs. SNT), susceptible non-treated (SNT) – red box, susceptible treated (ST) – black circle and miltefosine resistant (R40) – blue diamond, of *L. (L.) donovani* by the three analytical techniques. **a**) and **b**) are scores plot of GC-MS normalized data (with internal standard C18:0 methyl ester), treatment ( $R^2=0.908$  and  $Q^2=0.828$ ) and resistance ( $R^2=0.960$  and  $Q^2=0.930$ ),

respectively. **c**) and **d**) are scores plot of LC-MS analyzed data, treatment ( $R^2=1.000$  and  $Q^2=0.778$ ) and resistance ( $R^2=0.997$  and  $Q^2=0.927$ ), respectively. **e**) and **f**) are scores plot of CE-MS analyzed data, treatment ( $R^2=1.000$  and  $Q^2=0.828$ ) and resistance ( $R^2=0.999$  and  $Q^2=0.841$ ), respectively. Six replicates of each group of samples were analyzed, except in the case R40 by GC-MS

landscape, especially for those metabolites belonging to the same metabolic pathway but with vast differences in their respective chemical structure, requiring different separation techniques as assessed in Fig 4.

In this respect, CE, based on the differential separation of charged species inside an electric field, is orthogonal to the other separation techniques [42]; the first metabolic fingerprinting in *Leishmania* using CE-MS has been recently

published by us [56]. Complementary information was obtained by GC-MS, where compound identification is based on database mass spectra, due the high reproducibility of the fragmentation patterns [44], and if required, was confirmed with standards.

Non-polar *Leishmania* metabolites detected by reverse phase (LC-MS) demonstrated the suitability of lipidomics for this study, although because an excellent lipidomic on this

**Table 1** Number of features and compounds found after pre-treatment and statistical analysis of *L. (L.) donovani* data, analyzed by GC-MS, LC-MS and CE-MS

Analytical Technique	After Alignment	After Filtering		Statistically Significant		Putative/Identified	
		ST vs. SNT	R40 vs. SNT	ST vs. SNT	R40 vs. SNT	ST vs. SNT	R40 vs. SNT
GC-MS*	34	18	25	7	13	7	12
LC-MS**	9613	1622	1714	467	925	12	20
CE-MS**	2959	349	441	145	224	29	47

SNT –susceptible non-treated, ST – susceptible treated and R40 – resistant

\*the number means identified metabolites

\*\*the number means features (masses)

matter was recently reported for MT in *L. (L.) donovani* [21], this work focused on the identification of polar compounds.

When compared to untreated parasites, MT causes a decrease in the levels of Arg, ornithine (Orn) and citrulline, all belonging to the arginine-polyamine pathway, as well as of glutamate and proline (Pro) (Fig 5, plotted with our data on MassTrix, a web tool for mass identification and pathway highlighting of metabolites on KEGG pathway maps) [59]. The opposite pattern appears in resistant parasites, where these metabolites, together with spermidine were increased. In the biosynthesis of trypanothione, the main responsible for thiol redox metabolism in *Leishmania*, glutathionyl-spermidine and trypanothione disulfide (TS2) increased on resistant parasites, while TS2 decreased on treated parasites (Table 2).

Polyamine biosynthetic pathway provides spermidine for trypanothione biosynthesis, via conjugation with glutathione to produce glutathionyl-spermidine and trypanothione, the main anti-oxidant of the parasites against host cell oxidative burst [67], although recently, the importance of glutathione as a substantial player in the overall redox power of the parasite has been proposed [68]. Interestingly, variation in total level and the reduced: oxidized ratio of trypanothione is a typical response in antimonial treatment [69], also detected in a CE metabolomic study [56], which is in tune with partial cross-resistance between these two drugs [61].

The intracellular content of arginine underwent a drop close to 85 % in treated parasites (Table 2, Fig 5). L-arginine accomplishes two major roles in *Leishmania*, as a biosynthetic precursor for polyamines and building block for protein biosynthesis [70]; as such, L-arginine uptake is carried out by dedicated transporters that sense its intra- and extracellular concentration [70, 71]. Under this role, MT-treated parasites either loose the capacity to sense intracellular pools of Arg, otherwise transport capacity is unable to reach an adequate intracellular level of Arg. The latter may be caused by the decrease in adenosine triphosphate (ATP) observed in treated parasites [24] or impairment of the transporter activity due to the new phospholipid composition of the plasma membrane in ST. In contrast, trypanothione, the ultimate metabolite of the

pathway underwent decay, while spermidine and glutathione maintained their levels in ST, which may suggest a feasible inhibition of the final biosynthetic steps of trypanothione or drainage of its intracellular pool. In any case, shortage of trypanothione will increase the vulnerability of the parasite to oxidative stress, caused by increased levels of ROS induced by MT [12], aggravated due to the inhibition of electron flow across the respiratory chain at the level of cytochrome oxidase [24] and impairment of mitochondrial ROS detoxification by the release of superoxide dismutase [23].

Ornithine decreased by a half, which could be due to *Leishmania* lacks a complete urea cycle [53], including the lack of ornithine carbamoyl transferase. Therefore we may surmise that the decrease in citrulline does not obey to the decrease of Orn, but it is directly linked to the decrease of arginine through NO production by nitric oxide synthase, as constitutive activity described in *Leishmania* [72, 73], although identification of the encoding gene resulted elusive to date.

S-adenosylmethionine (SAM), but not methionine (Met), decreased in ST (Table 2). The drop of ATP, the other substrate of the reaction catalyzed by methionine adenosyltransferase may account for this effect. Treatment of parasites with MT led to a variation in the levels of intracellular pools for many amino acids.

These are versatile metabolites in *Leishmania*: biosynthetic blocks for protein synthesis, precursors for other metabolites, organic osmolytes involved in cellular volume regulation and metabolic fuel for the bioenergetics of the parasite, with crucial importance under a deficient supply of monosaccharides [74]. Interestingly, 18 of the 20 proteinogenic amino acids were increased in R40 parasites (with the exception of glycine (Gly) and cysteine (Cys)). In ST parasites, aside from the dramatic drop in Arg, the levels of many free amino acids were modified; only L-tyrosine underwent a small increase, whereas others amino acids experienced moderate (alanine (Ala), valine (Val), Pro, phenylalanine (Phe), tryptophan (Trp), glutamic acid (Glu)) to important decrease (glutamine (Gln)). In other words, a scenario resembling amino acid



**Table 2** Compounds statistically significant (by t test and/or Jack Knife with p-value<0.05) identify by GC-MS, LC-MS and CE-MS for miltefosine treatment and resistance in *L. (L.) donovani*

Compound Name	Monoisotopic Mass (Da)	Molecular Formula	Mass error* (ppm)	% fold change		Analytical Technique	Confirmation (% Probability)	Biochemical Nature
				ST vs SNT p-value/VIP[1]	R40 vs SNT p-value/VIP[1]			
Piperidine	83.0735	C <sub>5</sub> H <sub>9</sub> N	6.03	-30.96 0.0411/1.1894	135.05 0.0433/0.5940	CE-MS	Putative (86.75)	Amines
Putrescine	88.1000	C <sub>4</sub> H <sub>12</sub> N <sub>2</sub>		139.85 0.0116/1.2252		GC-MS	Identified	Amines
Alanine/ Sarcosine/ Aminopropionic acid	89.0477	C <sub>3</sub> H <sub>7</sub> NO <sub>2</sub>	6.98	-23.25 0.0022/2.0520	95.2 0.0022/ 1.87662	CE-MS	Putative (99.02)	Amino acids, peptides and conjugates
Serine	105.0426	C <sub>3</sub> H <sub>7</sub> NO <sub>3</sub>			194.63 0.0031/1.1650	GC-MS	Identified	Amino acids, peptides and conjugates
Proline	115.0633	C <sub>5</sub> H <sub>9</sub> NO <sub>2</sub>	-2.86	-19.51 0.0492/1.3138	135.49 0.0021/2.0481	CE-MS	Putative (98.64)	Amino acids, peptides and conjugates
Valine/ Betaine/ 5-Aminopentanoate/ 5-Aminopentanoic acid/ 4-Methylaminobutyrate	117.0790	C <sub>5</sub> H <sub>11</sub> NO <sub>2</sub>	0.18	-23.96 0.0151/1.7040	100.54 0.0022/0.1934	CE-MS	Putative (99.97)	Amino acids, peptides and conjugates
Threonine	119.0582	C <sub>4</sub> H <sub>9</sub> NO <sub>3</sub>	-2.04		89.05 0.0087/1.3606	CE-MS	Putative (47.58)	Amino acids, peptides and conjugates
					132.92 0.0249/0.9856	GC-MS	Identified	
4-Oxoproline/ L-1-Pyrroline- 3-hydroxy-5-carboxylate	129.0426	C <sub>5</sub> H <sub>7</sub> NO <sub>3</sub>	-4.6	-40.9 0.0021/2.1933	191.33 0.0022/2.0178	CE-MS	Putative (99.99)	Amino acids, peptides and conjugates
Pipecolic acid/ 4-Acetylaminobutanol	129.0790	C <sub>6</sub> H <sub>11</sub> NO <sub>2</sub>	0.17		307.94 0.0195/0.5816	CE-MS	Putative (97.06)	Ketones and aldehydes
L-glutamatesemialdehyde/ N-acetyl- L-glutamate/ N-acetyl-beta-alanine/ 2-oxo-5-aminovalerate/ trans-4- hydroxy-L-proline/ 5-Aminolevulminate	131.0582	C <sub>5</sub> H <sub>9</sub> NO <sub>3</sub>	-1.86	-72.71 0.0411/1.6202	-73.39 0.0433/1.5442	CE-MS	Putative (98.03)	Amino acids, peptides and conjugates
Leucine/ Isoleucine/ 2-Amino-3- methylvaleric acid/ 6-Amino-hexanoate	131.0946	C <sub>6</sub> H <sub>13</sub> NO <sub>2</sub>	2.83		162.31 0.0281/0.6497	CE-MS	Putative (87.87)	Amino acids, peptides and conjugates
N-carbamoyl-sarcosine/ L-Asparagine/ 3-Ureidopropionate	132.0535	C <sub>4</sub> H <sub>8</sub> N <sub>2</sub> O <sub>3</sub>	-3.73		132.69 0.0411/1.1534	CE-MS	NC	Amino acids, peptides and conjugates
Ornithine	132.0899	C <sub>5</sub> H <sub>12</sub> N <sub>2</sub> O <sub>2</sub>	-0.59	-45.48 0.0021/2.2097	1709.8 0.0022/2.0482	CE-MS	Putative (99.94)	Amino acids, peptides and conjugates
Aspartic acid	133.0375	C <sub>4</sub> H <sub>7</sub> NO <sub>4</sub>	-3.82		100 0.0016/1.3491	GC-MS	Identified	
					108.56 0.0022/ 0.02235	CE-MS	Putative (99.71)	Amino acids, peptides and conjugates
Malic acid	134.0215	C <sub>4</sub> H <sub>6</sub> O <sub>5</sub>			789.4 0.0016/1.2907	GC-MS	Identified	Organic acids
2-Phenylacetamide	135.0684	C <sub>8</sub> H <sub>9</sub> NO	-3.06		288.74 0.0151/1.4681	CE-MS	Putative (87.10)	Amides
Spermidine	145.1579	C <sub>7</sub> H <sub>19</sub> N <sub>5</sub>	0.02		112.39 0.0411/0.19911	CE-MS	Putative (99.99)	Polyamines
Glutamine	146.0691	C <sub>5</sub> H <sub>10</sub> N <sub>2</sub> O <sub>3</sub>			1866.2 0.0016/ 1.17701	GC-MS	Identified	Amino acids, peptides and conjugates
					200.19 0.0021/ 2.02953	CE-MS	Putative (99.98)	
Lysine	146.1055	C <sub>6</sub> H <sub>14</sub> N <sub>2</sub> O <sub>2</sub>	-3.61	-40.66 0.0022/2.2073	82.17 0.0281/0.6173	CE-MS	Putative (99.88)	Amino acids, peptides and conjugates
Glutamic acid	147.0532	C <sub>5</sub> H <sub>9</sub> NO <sub>4</sub>	-1.07	-24.55 0.0022/1.1858	75.76 0.0022/0.2215	CE-MS	Putative (99.95)	Amino acids, peptides and conjugates

Table 2 (continued)

Compound Name	Monoisotopic Mass (Da)	Molecular Formula	Mass error* (ppm)	% fold change		Analytical Technique	Confirmation (% Probability)	Biochemical Nature
				ST vs.SNT p-value/VIP[1]	R40 vs.SNT p-value/VIP[1]			
Methionine	149.0511	C <sub>5</sub> H <sub>11</sub> NO <sub>2</sub> S	-0.33			GC-MS	Identified	Amino acids, peptides and conjugates
Arabinol/ Ribitol/ Xylitol	152.0685	C <sub>5</sub> H <sub>12</sub> O <sub>5</sub>		93.67	0.014/1.06334	GC-MS	Identified	Carbohydrates
Histidine	155.0695	C <sub>6</sub> H <sub>9</sub> N <sub>3</sub> O <sub>2</sub>	0.15	0.0411/1.4541	0.0326/1.0483	CE-MS	Putative (99.73)	Amino acids, peptides and conjugates
Imidazole lactate/ 4-Imidazole-5-propanoate	156.0535	C <sub>6</sub> H <sub>8</sub> N <sub>2</sub> O <sub>3</sub>	-3.15	-47.26	0.0222/2.0351	CE-MS	Putative (87.60)	Organic acids
N-gamma-acetyl(diaminobutyrate)/ D-Alanyl-D-alanine	160.0848	C <sub>6</sub> H <sub>12</sub> N <sub>2</sub> O <sub>3</sub>	1.3	-23.79	143.87	CE-MS	Putative (86.84)	Amino acids, peptides and conjugates
Phenylalanine	165.0790	C <sub>9</sub> H <sub>9</sub> NO <sub>2</sub>	0.13	-13.75	0.0258/0.7117	CE-MS	Putative (99.98)	Amino acids, peptides and conjugates
4-Hydroxyphenylglyoxylate/ Phthalic acid	166.0266	C <sub>8</sub> H <sub>6</sub> O <sub>4</sub>	2.36	0.0087/1.5611	0.0259/1.2782	LC-MS	Putative (85.54)	Organic acids
Decanoic acid	172.1463	C <sub>10</sub> H <sub>20</sub> O <sub>2</sub>	-1.92	-47.26	0.0087/0.9701	LC-MS	Putative (79.15)	Fatty acids
N-acetylmethine	174.1004	C <sub>7</sub> H <sub>14</sub> N <sub>2</sub> O <sub>3</sub>	-2.54	0.0022/2.2180	0.0022/1.7575	CE-MS	Putative (99.72)	Amino acids, peptides and conjugates
Arginine	174.1117	C <sub>6</sub> H <sub>14</sub> N <sub>4</sub> O <sub>2</sub>	-3.88	-13.75	0.0481/1.1840	CE-MS	Putative (99.71)	Amino acids, peptides and conjugates
Citrulline	175.0957	C <sub>6</sub> H <sub>13</sub> N <sub>3</sub> O <sub>3</sub>	0.05	0.0087/1.5611	0.0411/0.9362	CE-MS	Putative (99.68)	Amino acids, peptides and conjugates
Myo-inositol	180.0634	C <sub>6</sub> H <sub>12</sub> O <sub>6</sub>		-97.45	81.98	GC-MS	Identified	Carbohydrates
Tyrosine	181.0739	C <sub>9</sub> H <sub>9</sub> NO <sub>3</sub>	-0.59	2.09	0.0062/1.0414	CE-MS	Putative (99.86)	Amino acids, peptides and conjugates
Indolepyruvic acid	187.0633	C <sub>11</sub> H <sub>9</sub> NO <sub>2</sub>	-1.76	-58.86	0.0261/0.0608	CE-MS	Putative (87.14)	Organic acids
N2-acetyl-L-lysine	188.1161	C <sub>8</sub> H <sub>16</sub> N <sub>2</sub> O <sub>3</sub>	-0.49	0.0411/1.4610	0.0411/1.0825	CE-MS	Putative (87.58)	Amino acids, peptides and conjugates
7,8-Diaminononanoate/ Trimethyl-L-lysine	188.1525	C <sub>9</sub> H <sub>20</sub> N <sub>2</sub> O <sub>2</sub>	-4.13	-79.39	0.0411/0.7916	CE-MS	Putative (85.57)	Amino acids, peptides and conjugates
N-carbamyl-L-glutamate	190.0590	C <sub>6</sub> H <sub>10</sub> N <sub>2</sub> O <sub>5</sub>	0.15	0.0021/1.9680	0.0022/1.7158	CE-MS	NC	Amino acids, peptides and conjugates
2,6-Diaminoheptanedioate	190.0954	C <sub>7</sub> H <sub>14</sub> N <sub>2</sub> O <sub>4</sub>	3.38	-22.46	0.0281/1.2268	CE-MS	Putative (87.17)	Amines and organic acids
Dodecanoic acid	200.1776	C <sub>12</sub> H <sub>24</sub> O <sub>2</sub>	-3.15	-54.02	0.0259/1.2309	LC-MS	Putative (92.95)	Fatty acids
Tryptophane	204.0899	C <sub>11</sub> H <sub>12</sub> N <sub>2</sub> O <sub>2</sub>	0.6	-20.65	0.0411/1.8310	CE-MS	Putative (99.87)	Amino acids, peptides and conjugates
N-acetyl-N-hydroxy-L-lysine	204.1110	C <sub>8</sub> H <sub>16</sub> N <sub>2</sub> O <sub>4</sub>	-4.93	0.0411/1.3087	0.0411/1.2385	CE-MS	Putative (86.78)	Amino acids, peptides and conjugates
gamma-L-Glutamylputrescine/ beta-Alanyl-L-lysine	217.1426	C <sub>9</sub> H <sub>19</sub> N <sub>3</sub> O <sub>3</sub>	0.73	-29.73	0.0043/1.6192	CE-MS	Putative (99.25)	Amino acids, peptides and conjugates
N2-(D-1-carboxyethyl)-L-lysine	218.1267	C <sub>9</sub> H <sub>18</sub> N <sub>2</sub> O <sub>4</sub>	-3.01	-22.89	0.0411/1.0498	CE-MS	Putative (87.14)	Amino acids, peptides and conjugates
Cystathionine	222.0674	C <sub>7</sub> H <sub>14</sub> N <sub>2</sub> O <sub>4</sub> S	0.77	0.0393/1.2757	0.0411/1.1516	CE-MS	Putative (99.82)	Amino acids, peptides and conjugates
2,5-Dichloro-4-oxohex-2-enedioate	225.9436	C <sub>6</sub> H <sub>4</sub> Cl <sub>2</sub> O <sub>5</sub>	1.87	-48.58	0.0022/2.0298	CE-MS	NC	Organochlorines
				0.0151/1.4513	-39.83			

Table 2 (continued)

Compound Name	Monoisotopic Mass (Da)	Molecular Formula	Mass error* (ppm)	% fold change		Analytical Technique	Confirmation (% Probability)	Biochemical Nature
				ST vs.SNT p-value/ViP[1]	R40 vs.SNT p-value/ViP[1]			
Carnosine	226.1066	C <sub>8</sub> H <sub>14</sub> N <sub>4</sub> O <sub>3</sub>	-2.61		146.28 0.0259/0.7885	Putative (81.39)	Amino acids, peptides and conjugates	
Tetradecanoic acid (Myristic acid)	228.2089	C <sub>14</sub> H <sub>28</sub> O <sub>2</sub>			1248.5 0.0016/1.4016	Identified	Fatty acids	
2-Oxo-10-methylthiostearic acid	232.1133	C <sub>11</sub> H <sub>20</sub> O <sub>3</sub> S	-1.36		52 0.0411/1.3116	NC	Thiocarboxylic acids	
beta-Alanyl-L-arginine	245.1488	C <sub>9</sub> H <sub>19</sub> N <sub>5</sub> O <sub>3</sub>	-3.22		180.55 0.0152/0.1864	Putative (86.44)	Amino acids, peptides and conjugates	
Subaphyllin	264.1474	C <sub>14</sub> H <sub>20</sub> N <sub>2</sub> O <sub>3</sub>	-1.86	-21.69	181.64 0.0770/1.4363	Putative (86.61)	Alkaloids	
Heptadecatrienoic acid	264.2089	C <sub>17</sub> H <sub>28</sub> O <sub>2</sub>	-3.52	0.0493/1.2162	549.45 0.0022/1.7148	Putative (90.95)	Fatty acids	
Octadecatrienoic acid (Stearidonic acid)	276.2089	C <sub>18</sub> H <sub>32</sub> O <sub>2</sub>	0.25	-32.01	376.11 0.0043/1.8281	Putative (97.21)	Fatty acids	
Octadecatrienoic acid (linolenic acid)	278.2246	C <sub>18</sub> H <sub>30</sub> O <sub>2</sub>	-2.09	64.18 0.026/0.82581	64.12 0.0022/1.8229	109,1002, 123,1150, 135,1153, 149, 1327, 173,1262, 191,1747, 205,1891	Fatty acids	
Octadecadienoic acid (Linoleic acid)	280.2402	C <sub>18</sub> H <sub>32</sub> O <sub>2</sub>		69.24 0.0043/1.3001	38.13 0.0022/1.7672	Identified	Fatty acids	
Octadecenoic acid (Oleic acid)	282.2559	C <sub>18</sub> H <sub>34</sub> O <sub>2</sub>		61.39 0.0433/1.1344		135,1173, 149,1334, 161,1316, 175,1478, 245,2274	Fatty acids	
Octadecanoic acid (Stearic acid)	284.2715	C <sub>18</sub> H <sub>36</sub> O <sub>2</sub>		48.52 0.0086/1.2210		Identified	Fatty acids	
Abietinol/ Kaur-16-en-18-ol/ Neobietinol/ Levopimarino	288.2453	C <sub>30</sub> H <sub>42</sub> O	5.84		-52.53 0.0216/0.02661	Putative (67.25)	Diterpenoids	
Sphingosine	299.2824	C <sub>18</sub> H <sub>37</sub> NO <sub>2</sub>	-4.78	53.12 0.0411/0.7724	0.98 0.0411/0.9856	135,1155, 149,1265, 211,2063, 252,2695, 253,2723, 264,2682, 265,2647, 282,2814, 282,3958, 283,2854	Sphingolipids and spingoid bases	
Sphinganine	301.2981	C <sub>18</sub> H <sub>39</sub> NO <sub>2</sub>	-0.26		-63.46 0.0022/0.8462	Putative (85.55)	Sphingolipids and spingoid bases	
Icosatetraenoic acid	304.2402	C <sub>20</sub> H <sub>32</sub> O <sub>2</sub>	5.82		96.5 0.0043/1.6704	Putative (79.07)	Fatty acids	
Docosahexaenoic acid	328.2402	C <sub>22</sub> H <sub>32</sub> O <sub>2</sub>	2.35		78.33 0.0259/1.5792	107,1002, 135,1153, 147,1155, 161,1316, 175,1486, 215,1767, 269,2271, 293,2273, 311,2354	Fatty acids	
Docosapentaenoic acid	330.2559	C <sub>22</sub> H <sub>34</sub> O <sub>2</sub>	6.42		17.72 0.0087/1.3158	Putative (77.43)	Fatty acids	
Lobeline	337.2042	C <sub>22</sub> H <sub>27</sub> NO <sub>2</sub>	-6.46	203.77 0.0022/1.8029		Putative (81.45)	Alkaloids	
Thiamine monophosphate	345.0786	C <sub>12</sub> H <sub>18</sub> N <sub>4</sub> O <sub>4</sub> PS	-5.27	1293.1 0.0433/0.6150		NC	Phosphate derivatives	
cis/trans-Zeaxin riboside	351.1543	C <sub>15</sub> H <sub>21</sub> N <sub>4</sub> O <sub>5</sub>	4.93	227.09 0.0043/1.7099		Putative (76.13)	Cytokinins	
Cholesterol	386.3549	C <sub>27</sub> H <sub>46</sub> O				Identified	Sterols	

Table 2 (continued)

Compound Name	Monoisotopic Mass (Da)	Molecular Formula	Mass error* (ppm)	% fold change		Analytical Technique	Confirmation (% Probability)	Biochemical Nature
				ST vs. SNT p-value/VIP[1]	R40 vs. SNT p-value/VIP[1]			
LPA(P-16:0e/0:0)	394.2484	C <sub>19</sub> H <sub>39</sub> O <sub>4</sub> P	-3.62	46.87	333.07	LC-MS	Putative (68.31)	Glycerophospholipids
Ergosterol	396.3392	C <sub>28</sub> H <sub>44</sub> O		0.0411/1.1261	24.74			
S-Adenosyl-L-methionine (SAMe)	398.1372	C <sub>15</sub> H <sub>22</sub> N <sub>6</sub> O <sub>5</sub> S	1.41	-51.83	0.0411/1.3333	GC-MS	Identified	Sterols and prenol lipids
S-Glathionyl-L-cysteine	426.0879	C <sub>13</sub> H <sub>22</sub> N <sub>4</sub> O <sub>6</sub> S <sub>2</sub>	-0.48	0.0059/1.7128	0.0143/1.1706	CE-MS	Putative (71.91)	Amino acids, peptides and conjugates
Glutathionylspermidine	434.2311	C <sub>17</sub> H <sub>34</sub> N <sub>6</sub> O <sub>5</sub> S	-0.32	-30.11	73.24	CE-MS	NC	Amino acids, peptides and conjugates
Leukotriene D4	496.2607	C <sub>25</sub> H <sub>40</sub> N <sub>2</sub> O <sub>6</sub> S	-3.44	0.0022/1.9213	0.0411/0.8386	CE-MS	NC	Amino acids, peptides and conjugates
L-Oleandrosyl-oleandrolide	530.3091	C <sub>27</sub> H <sub>46</sub> O <sub>10</sub>	0	0.0022/1.8360	738.22	CE-MS	NC	Amino acids, peptides and conjugates
PC(0-18:(10E)/2:0)	549.3794	C <sub>38</sub> H <sub>56</sub> NO <sub>2</sub> P	1.02	388.56	0.0411/0.6039	CE-MS	NC	Lactone polyketides
N-acetyl-N6,0-didemethylpuromycin-5'-phosphate	565.1686	C <sub>22</sub> H <sub>28</sub> N <sub>4</sub> O <sub>8</sub> P	-6.39	0.0151/0.9281	25.45	LC-MS	NC	Fatty acids derivatives
PC(22-4(7Z,10Z,13Z,16Z)/0:0)	571.3638	C <sub>30</sub> H <sub>54</sub> NO <sub>2</sub> P	-1.74	0.15461	179.23	CE-MS	NC	Lactone polyketides
PC(22:(11Z)/0:0)	577.4107	C <sub>30</sub> H <sub>60</sub> NO <sub>2</sub> P	0.33	0.0411/0.6790	-28.77	LC-MS	Putative (99.43)	Glycerophospholipids
CMP-N-acetylneuraminic acid	614.1473	C <sub>20</sub> H <sub>31</sub> N <sub>4</sub> O <sub>16</sub> P	2.82	54.84	0.0022/0.9949	LC-MS	NC	Acetyl derivatives
Dihydrostreptomycin 6-phosphate	663.2477	C <sub>27</sub> H <sub>42</sub> N <sub>7</sub> O <sub>15</sub> P	-4.00	0.0158/1.9355	179.23	LC-MS	NC	Acetyl derivatives
Phosphatidic acid	674.4886	C <sub>37</sub> H <sub>71</sub> O <sub>8</sub> P	-6.9	-14.46	0.0411/0.3448	LC-MS	Putative (99.12)	Glycerophospholipids
Trypanothione disulfide	721.2887	C <sub>27</sub> H <sub>47</sub> N <sub>9</sub> O <sub>10</sub> S <sub>2</sub>	-1.01	72.71	0.0022/1.9953	LC-MS	Putative (97.51)	Glycerophospholipids
Megalomicin A	876.5558	C <sub>44</sub> H <sub>80</sub> N <sub>2</sub> O <sub>15</sub>	0.15	-73.59	0.0022/1.7301	LC-MS	NC	Acetyl derivatives
				0.0043/1.9306	-96.28	LC-MS	NC	Lactone polyketides
				0.0411/1.3483	-96.76	LC-MS	NC	Lactone polyketides
				0.0411/0.0566	340.58	LC-MS	NC	Phospholipids
				46.38	0.0086/0.9807	CE-MS	Putative (82.8)	Amino acids, peptides and conjugates
				3.74		LC-MS	NC	Lactone polyketides
				0.0151/1.2435				

Separation and detection conditions are described in Materials and Methods

NC – not confirmed, SNT –susceptible non-treated, ST – susceptible treated and R40 – resistant

\*Mass error is related to differences between the equipments (LC-MS and CE-MS) and the public database search

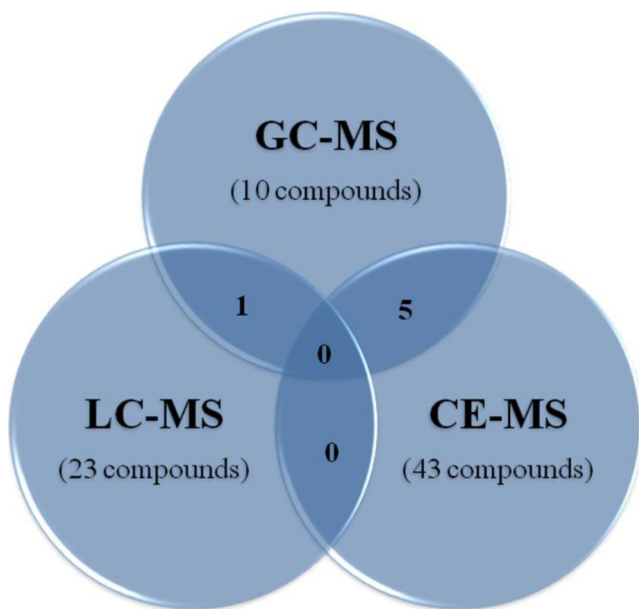


**Fig. 4** Venn diagram comparing the significant and identified compounds by the three analytical platforms

starvation was created by MT; despite the strong capability of amino acid inter conversion in *Leishmania* afforded by the tricarboxylic acid cycle (TCA) and aminotransferases, this amino acid shortage may impair the rate of protein synthesis, however if so, it is puzzling that other essential amino acids such as lysine [75] or the aforementioned methionine [76], did not undergo variation. Importantly, none of the Ser (serine)/Gly/Cys triad, also connected to methionine biosynthesis through homocysteine underwent significant variation. These three amino acids are metabolically related by pathways outside the anaplerotic TCA, evidencing the high interconversion plasticity of this set of amino acids.

Amino acids, especially Asp in *Leishmania*, play an important role in metabolism; transaminases convert Glu and Asp (asparagines) to Ala with  $\alpha$ -ketoglutarate, oxaloacetate and pyruvate, all of which are substrates for TCA once inside the mitochondria facilitated by a specific mitochondrial transporter or, for oxoglutarate, after their conversion into malate [74]. Glu and Gln underwent a moderate decreases in ST. A specific transporter for glutamate has been described in

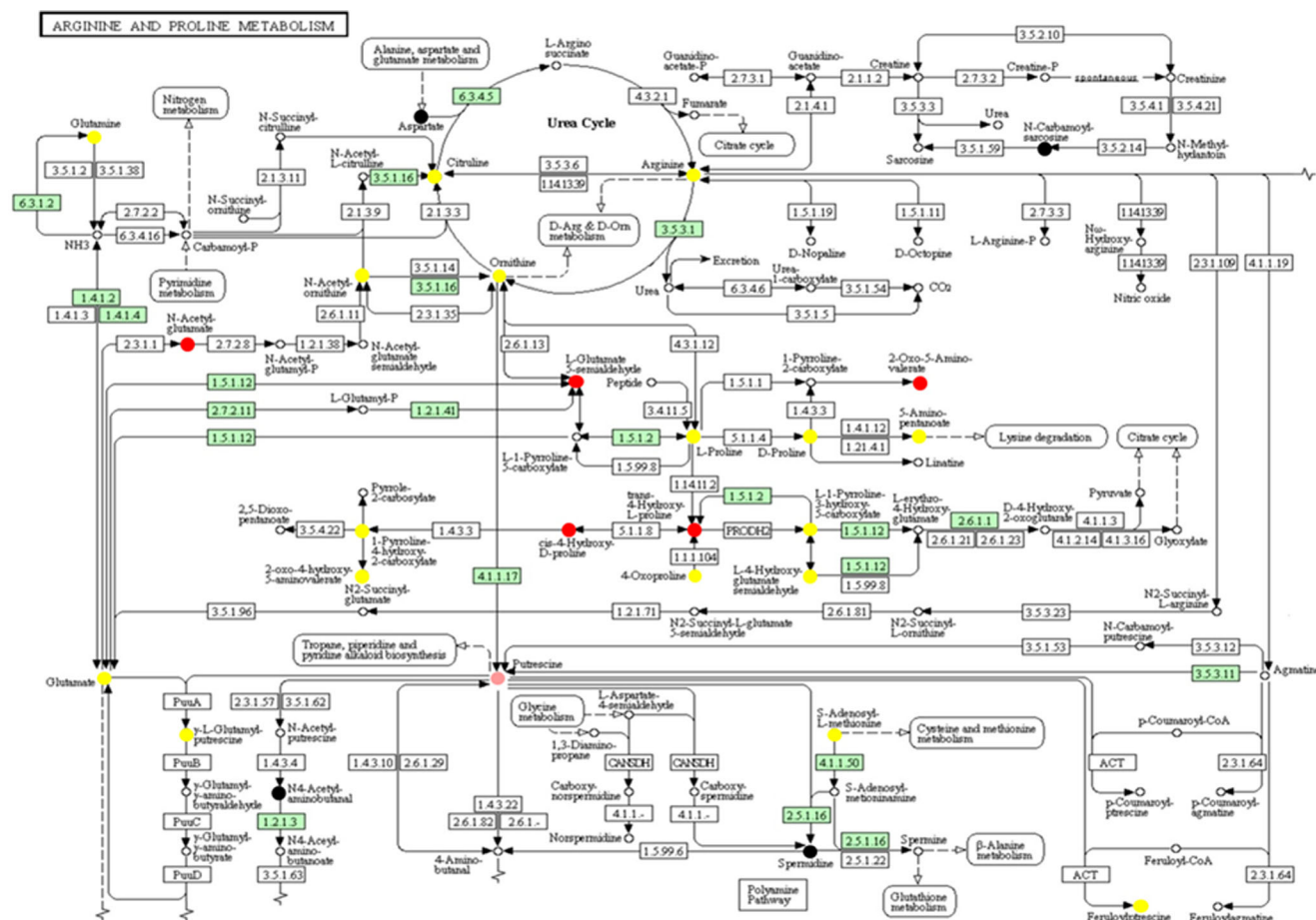


**Fig. 5** Arginine and proline metabolic pathway showing compound that significantly changed in miltefosine treatment of *L. (L.) donovani*. Dot color represent our treatment response: red – decreased both ST and R40, yellow – decreased on ST and increased on R40, pink – increased only on

ST and black – increased only on R40. Green boxes represent enzymes already annotated in the parasite. (ST –susceptible non-treated and R40 – resistant). Font: MassTrix - <http://metabolomics.helmholtz-muenchen.de/masstrix2/> [59]

*Leishmania* dependent on  $K^+$  gradients across the membrane [77]; hence if this gradient is collapsed by membrane leakage and/or shortage of bioenergetic fuel for ionic pumps [24], the Glu level will decrease. Pro, the other precursor for Glu also decreased which could also explain the increased metabolism of Glu. In fact it has been reported that only 30 % of the overall Glu uptake is incorporated in proteins [77], so here it could be involved with  $\alpha$ -ketoglutarate to replenish the mitochondrial TCA directly by glutamate dehydrogenase, or by transamination with pyruvate to produce Ala.

Interestingly, variation in the levels of different sugars were scarcely present; ST parasites showed an increase of a metabolite whose mass matches that of ribitol, and its isomers arabitol or xylitol (Table 2). In any case all of them arise as degradation products for D-ribulose 5-phosphate by pentose interconversion, connected to the activity of the pentose phosphate pathway, located in the glycosome in *Leishmania* [78]. This is a route that not only supplies pentose nucleosides, but also provides redox equivalents which help to cope with oxidative stress, enhanced by MT.

From lipidomic results, obtained by other groups, the strong restructuration of membrane architecture was highlighted. In this regard, the decrease in S-adenosylmethionine, may not only jeopardize spermidine biosynthesis, commented previously, but also, since it works as a methyl group donor through SAM-dependent methylases, including phosphatidylethanolamine N-methyltransferase, this deficiency may contribute partially to the formation of phosphatidylcholine. Accordingly, the decrease in S-adenosylmethionine, together with the decrease in choline transport mediated by MT [18], as precursor for cytidine diphosphate-choline (CDP-choline), may underline the inversion of PE:PC ratio in MT-treated parasites.

Interestingly, in MT treated parasites, the ergosterol content is known to be halved with respect to control parasites, as described previously [22]. In our experiment however, none of the ergosterol precursors were detected, including leucine(Leu)/isoleucine(Ile), that provides the carbon skeleton for the synthesis of ergosterol [79]. Farnesol has not been described in *Leishmania*, so it may proceed from the hydrolysis of its diphosphate form.

Fatty acids may be involved in the biosynthesis of sphingolipids as well as in phospho-, glycerol- and ether-lipids, and also important bioenergetic fuel for *Leishmania* through their  $\beta$ -oxidation.

Among trypanosomatids, *Leishmania* possesses the highest capacity for synthesis and modification of unsaturated fatty acids, with an extensive repertoire of elongases and of front-end and methyl- fatty acid desaturases [80]. The MT-treated parasites showed an increase in the fatty acids amines (FAA) pathway: stearic  $\rightarrow$  oleic  $\rightarrow$  linoleic  $\rightarrow$  linolenic acid. Only octadecatetraenoic acid decreased. In contrast,

docosatetraenoic acid, derived from linoleic acid, was increased.

From these results, we may infer two conclusions: first, the ratio between *n*-6:*n*-3 unsaturated fatty acid was rather preserved as both linoleic- and linolenic-derived FAA increased in the same direction [80]. Secondly, the decrease in octadecatetraenoic acid would suggest  $\Delta$ -6-desaturase as a feasible target for MT, as the concentration of linolenic acid, its immediate upstream precursor, increases.

The identification of 12-oXoEte a leukotriene that underwent a decrease in ST parasites is interesting with respect to the fact that biosynthesis of prostaglandins in *Leishmania* has been reported by functional assays or inferred from proteomic identification of their biosynthetic enzymes, but to the best of our knowledge none leukotriene has been described. Their precursor metabolite, arachidonic acid, will be available by phospholipase A<sub>2</sub> activity, although, one close ortholog for lipooxygenase, the first enzyme in leukotriene synthesis has been reported in *Leishmania* genome. Confirmation by radioactive or mass isotopic labeling of arachidonic acid will be carried out, in order to assess whether new biosignalling lipids are produced by *Leishmania*, and if part of the chemotherapeutic activity of miltefosine may rely on the modification of their levels.

The most appealing fact in the resistant strain is the increase of the intracellular concentration of many amino acids, in some cases accompanied by downstream products in their respective metabolic pathways. The protein content will be under strict control for parasites. So protein degradation will be ruled out as the origin for this increase. Other amino acid degradation metabolites, such as indolpyruvate (from Trp), imidazol lactate (from histidine (His)), oxoproline (from Pro), or 2-phenylacetamide (from Phe) also showed modified levels.

The outstanding increase of Asp levels provided evidence for its role as key metabolite for *Leishmania* both as a substrate for aminotransferases or as a precursor for malic acid and pyruvate. Its role as an anaplerotic metabolite for TCA cycle was assessed even under glucose-depleted conditions in *L. mexicana* [74].

*Leishmania* senses intracellular pools at least for Arg [71] and Pro [81] with crossed-influence between these metabolites. In this sense, Inbard *et al.* [81] proposed recently an appealing hypothesis consisting of the cross-talk among the different amino acid transporters through their large hydrophilic N-terminal extension, typical in *Leishmania*, which will be modulated allosterically by these amino acids. A suggestive hypothesis is whether the interaction of this tail with the membrane will explore different membrane architectures in the parasite created by dysfunction of the MT transporter [82]. Some trends can be detected for free fatty acids anions (FFAA) in R40 parasites. For example, the presence of medium length saturated FFAA was decreased, whereas stearic acid

and its polyunsaturated fatty acids (PUFA) derived surrogates increased. Also PUFA families of higher chain length as icosanoic and docosanoic acid were decreased.

A straightforward extrapolation of our data into the intracellular stage is a risky process, firstly because of the significant metabolic differences between amastigotes and promastigotes, for instance, where for promastigotes there is a higher importance for amino acid and fatty acid oxidation as well as of hexosamine metabolism for energy requirements; and secondly, because nutrient levels available to the intracellular parasite inside the parasitophorous vacuole are to a great extent unknown. In most cases these are inferred from the survival and virulence for parasites crippled in a gene encoding an enzyme essential for a given pathway (reviewed in [51, 52, 83]).

In essence, the most important finding on our work is the lower capacity of ST parasites to hold a sustained defense to oxidative stress. For intracellular parasites, this scenario will be worsened; first because oxidative stress is high inside the phagosome [84], and secondly because a higher intrinsic ROS production is expected in the amastigote, due to the higher mitochondrial activity, increased by the blockage of the cytochrome oxidase of the respiratory chain by miltefosine [24]. Additional dysfunction of mitochondria can be expected by the severe reduction of ergosterol observed for ST, in some way mimicking the effect of inhibitors of ergosterol biosynthesis to which amastigotes are remarkably susceptible [85].

At the other side of the scale stand the metabolic defenses of the parasite against oxidative stress. Amastigotes are well adapted to thrive under this hostile environment since they have a robust superoxide dismutase system, capacity to reduce ascorbic acid, and a redox system based on trypanothione, that are essential for this task. ST promastigotes showed a drastic decrease over SNT in their arginine and polyamine content, as precursors for spermidine biosynthesis, needed for trypanothione biosynthesis. Unexpectedly, despite the abundance of amino acids as end-products of proteolytic degradation inside the phagosome, arginine is a limiting nutrient as evidenced by the impaired infectivity of knock-out parasites for arginase in animal models [86]. Even though components of the triad Ser/Gly/Cys remained at similar levels between SNT and ST promastigotes, Cys and Gly are two metabolites requiring salvage from external supply for intracellular amastigotes [52], so shortage for trypanothione precursor will be even worse than on promastigotes. It is worth mentioning that the lower rate of proliferation for amastigotes, may alleviate these requirements.

Furthermore, if the general decrease in amino acid levels observed in promastigotes is maintained in amastigotes, it will suppose a decreased supply of substrates throughout the TCA. As glycolysis is diminished in this stage, a feasible decrease of the capacity to generate ATP will ensue. A constant supply of ATP is needed in order to maintain the  $H^+$  gradient across the plasma membrane of the parasite, required for maximal functionality of many amastigote transporters [87].

## Conclusions

We have demonstrated the robustness of metabolomics as a powerful tool to open new avenues in the understanding of mechanism of drug action and resistance in *Leishmania*. Using three different separation techniques, with CE as an orthogonal technique to the other two chromatographic strategies, we unraveled unexpected changes in metabolic adaptation to a priori minimalistic mechanism of resistance to MT, such as the denial of drug uptake by the parasite.

Impairment of the pathway Arginine  $\rightarrow$  polyamine trypanothione in susceptible parasites treated with MT was in some way expected, considering the ROS production described for MT. Importantly, in resistant parasites an increase in the levels of amino acids was the most outstanding feature. Although the physiological meaning underlying these changes remains unclear, the high versatility of amino acids in *Leishmania* provided by their flow through TCA and amino-transferases must be kept in mind [88]. This also poses the question of metabolic adaptation of the resistant strain, which apparently preserves its fitness inside the parasitophorous vacuole, where it is envisaged a limiting supply of amino acids.

Our results confirm the feasibility of partial cross-resistance for antimonials and MT, as both mechanisms share a decrease in trypanothione-dependent redox capacity of the parasite [56]. In this sense, new inhibitors of the polyamine pathway or of redox metabolism of trypanothione will be good candidates for drug combination with miltefosine, or even to work as revertants of resistance. We may also surmise that the deterioration of TCA cycle will likely lead to a synergic effect of MT with other drugs targeting enzymes of the TCA cycle, such as licochalcones that act as inhibitors of fumarate reductase [89], or in other complexes of the respiratory chain, aside from the cytochrome c oxidase as the target for MT. In this sense sitamaquine, acting on succinate dehydrogenase [90] will be a feasible candidate, opening new alternatives to the alarming reduction of drugs against *Leishmania*.

Several caveats underlined the previous comments; firstly this study is based on a static snapshot of *Leishmania* metabolism. Many of the hypotheses mentioned before prompt studies with metabolic precursors containing stable carbon isotopes, in order to carry out kinetic metabolomic studies to assess the buildup or decrease of metabolite pools, as demonstrated recently by Saunders *et al.* [74], 2011.

**Acknowledgments** This work was supported by grants from Spanish Ministry of Science and Innovation (MICINN CTQ2011-23562) (CB), FIS PS09-01928 and PI12-02706, (LR) EADS-CASA and Brazilian Air Force (FAB). (CB) L.R. belongs to the Red de Investigación Cooperativa en Enfermedades Tropicales (RICET) RD 06/0021/0006 and RD12/0018/0007. G. A. B. C. is thankful to FAPESP for a doctoral fellowship.

## References

- Organization WH Technical report series no. 949. In: Control of the leishmaniasis: report of a meeting of the World Health Organization Expert Committee on the Control of Leishmaniases, Geneva, 2010. pp 22–26
- Alvar J, Vélez ID, Bern C, Herrero M, Desjeux P, Cano J, Jannin J, den Boer M, Team WLC (2012) Leishmaniasis worldwide and global estimates of its incidence. *PLoS One* 7(5):e35671
- Alvar J, Croft SL, Kaye P, Khamesipour A, Sundar S, Reed SG (2013) Case study for a vaccine against leishmaniasis. *Vaccine* 31(Suppl 2):B244–B249
- Nagill R, Kaur S (2011) Vaccine candidates for leishmaniasis: a review. *Int Immunopharmacol* 11(10):1464–1488
- Croft SL, Olliaro P (2011) Leishmaniasis chemotherapy—challenges and opportunities. *Clin Microbiol Infect* 17(10):1478–1483
- van Griensven J, Balasegaram M, Meheus F, Alvar J, Lynen L, Boelaert M (2010) Combination therapy for visceral leishmaniasis. *Lancet Infect Dis* 10(3):184–194
- Sundar S, Chakravarty J (2013) Leishmaniasis: an update of current pharmacotherapy. *Expert Opin Pharmacother* 14(1):53–63
- Alvar J, Yactayo S, Bern C (2006) Leishmaniasis and poverty. *Trends Parasitol* 22(12):552–557
- Sundar S, Jha TK, Thakur CP, Engel J, Sindermann H, Fischer C, Junge K, Bryceson A, Berman J (2002) Oral miltefosine for Indian visceral leishmaniasis. *N Engl J Med* 347(22):1739–1746
- Dorlo TP, Balasegaram M, Beijnen JH, de Vries PJ (2012) Miltefosine: a review of its pharmacology and therapeutic efficacy in the treatment of leishmaniasis. *J Antimicrob Chemother* 67(11):2576–2597
- Kumar D, Kulshrestha A, Singh R, Salotra P (2009) In vitro susceptibility of field isolates of *Leishmania donovani* to Miltefosine and amphotericin B: correlation with sodium antimony gluconate susceptibility and implications for treatment in areas of endemicity. *Antimicrob Agents Chemother* 53(2):835–838
- Moreira W, Leprohon P, Ouellette M (2011) Tolerance to drug-induced cell death favours the acquisition of multidrug resistance in *Leishmania*. *Cell Death Dis* 2:e201
- Rijal S, Ostyn B, Uranw S, Rai K, Bhattarai NR, Dorlo TP, Beijnen JH, Vanaershot M, Decuypere S, Dhakal SS, Das ML, Karki P, Singh R, Boelaert M, Dujardin JC (2013) Increasing failure of miltefosine in the treatment of Kala-azar in Nepal and the potential role of parasite drug resistance, reinfection, or noncompliance. *Clin Infect Dis* 56(11):1530–1538
- Sundar S, Chakravarty J (2012) Recent advances in the diagnosis and treatment of kala-azar. *Natl Med J India* 25(2):85–89
- Paris C, Loiseau PM, Bories C, Bréard J (2004) Miltefosine induces apoptosis-like death in *Leishmania donovani* promastigotes. *Antimicrob Agents Chemother* 48(3):852–859
- Proto WR, Coombs GH, Mottram JC (2013) Cell death in parasitic protozoa: regulated or incidental? *Nat Rev Microbiol* 11(1):58–66
- Saugar JM, Delgado J, Homillos V, Luque-Ortega JR, Amat-Guerri F, Acuña AU, Rivas L (2007) Synthesis and biological evaluation of fluorescent leishmanicidal analogues of hexadecylphosphocholine (miltefosine) as probes of antiparasite mechanisms. *J Med Chem* 50(24):5994–6003
- Zufferey R, Mamoun CB (2002) Choline transport in *Leishmania major* promastigotes and its inhibition by choline and phosphocholine analogs. *Mol Biochem Parasitol* 125(1–2):127–134
- Lux H, Heise N, Klenner T, Hart D, Opperdoes FR (2000) Ether-lipid (alkyl-phospholipid) metabolism and the mechanism of action of ether-lipid analogues in *Leishmania*. *Mol Biochem Parasitol* 111(1):1–14
- Barratt G, Saint-Pierre-Chazalet M, Loiseau PM (2009) Cellular transport and lipid interactions of miltefosine. *Curr Drug Metab* 10(3):247–255
- Imbert L, Ramos RG, Libong D, Abreu S, Loiseau PM, Chaminade P (2012) Identification of phospholipid species affected by miltefosine action in *Leishmania donovani* cultures using LC-ELSD, LC-ESI/MS, and multivariate data analysis. *Anal Bioanal Chem* 402(3):1169–1182
- Rakotomanga M, Saint-Pierre-Chazalet M, Loiseau PM (2005) Alteration of fatty acid and sterol metabolism in miltefosine-resistant *Leishmania donovani* promastigotes and consequences for drug-membrane interactions. *Antimicrob Agents Chemother* 49(7):2677–2686
- Getachew F, Gedamu L (2012) *Leishmania donovani* mitochondrial iron superoxide dismutase A is released into the cytosol during miltefosine induced programmed cell death. *Mol Biochem Parasitol* 183(1):42–51
- Luque-Ortega JR, Rivas L (2007) Miltefosine (hexadecylphosphocholine) inhibits cytochrome c oxidase in *Leishmania donovani* promastigotes. *Antimicrob Agents Chemother* 51(4):1327–1332
- Zuo X, Djordjevic JT, Bijosono Oei J, Desmarini D, Schibeci SD, Jolliffe KA, Sorrell TC (2011) Miltefosine induces apoptosis-like cell death in yeast via Cox9p in cytochrome c oxidase. *Mol Pharmacol* 80(3):476–485
- Das M, Saudagar P, Sundar S, Dubey VK (2013) Miltefosine-unresponsive *Leishmania donovani* has a greater ability than miltefosine-responsive *L. donovani* to resist reactive oxygen species. *FEBS J* 280(19):4807–4815
- Mishra J, Singh S (2013) Miltefosine resistance in *Leishmania donovani* involves suppression of oxidative stress-induced programmed cell death. *Exp Parasitol* 135(2):397–406
- Pérez-Victoria FJ, Gamarro F, Ouellette M, Castanys S (2003) Functional cloning of the miltefosine transporter. A novel P-type phospholipid translocase from *Leishmania* involved in drug resistance. *J Biol Chem* 278(50):49965–49971
- Pérez-Victoria FJ, Castanys S, Gamarro F (2003) *Leishmania donovani* resistance to miltefosine involves a defective inward translocation of the drug. *Antimicrob Agents Chemother* 47(8):2397–2403
- Pérez-Victoria FJ, Sánchez-Cañete MP, Castanys S, Gamarro F (2006) Phospholipid translocation and miltefosine potency require both *L. donovani* miltefosine transporter and the new protein LdRos3 in *Leishmania* parasites. *J Biol Chem* 281(33):23766–23775
- Sánchez-Cañete MP, Carvalho L, Pérez-Victoria FJ, Gamarro F, Castanys S (2009) Low plasma membrane expression of the miltefosine transport complex renders *Leishmania braziliensis* refractory to the drug. *Antimicrob Agents Chemother* 53(4):1305–1313
- Castanys-Muñoz E, Pérez-Victoria JM, Gamarro F, Castanys S (2008) Characterization of an ABCG-like transporter from the protozoan parasite *Leishmania* with a role in drug resistance and transbilayer lipid movement. *Antimicrob Agents Chemother* 52(10):3573–3579
- Pérez-Victoria JM, Pérez-Victoria FJ, Parodi-Talice A, Jiménez IA, Ravelo AG, Castanys S, Gamarro F (2001) Alkyl-lysophospholipid resistance in multidrug-resistant *Leishmania tropica* and chemosensitization by a novel P-glycoprotein-like transporter modulator. *Antimicrob Agents Chemother* 45(9):2468–2474
- Coelho AC, Boisvert S, Mukherjee A, Leprohon P, Corbeil J, Ouellette M (2012) Multiple mutations in heterogeneous miltefosine-resistant *Leishmania major* population as determined by whole genome sequencing. *PLoS Negl Trop Dis* 6(2):e1512
- Cojean S, Houzé S, Haouchine D, Huteau F, Lariven S, Hubert V, Michard F, Bories C, Pratlong F, Le Bras J, Loiseau PM, Matheron S (2012) *Leishmania* resistance to miltefosine associated with genetic marker. *Emerg Infect Dis* 18(4):704–706



36. Bhandari V, Kulshrestha A, Deep DK, Stark O, Prajapati VK, Ramesh V, Sundar S, Schonian G, Dujardin JC, Salotra P (2012) Drug susceptibility in *Leishmania* isolates following miltefosine treatment in cases of visceral leishmaniasis and post kala-azar dermal leishmaniasis. *PLoS Negl Trop Dis* 6(5):e1657
37. García-Hernández R, Manzano JJ, Castanys S, Gamarro F (2012) *Leishmania donovani* develops resistance to drug combinations. *PLoS Negl Trop Dis* 6(12):e1974
38. Xiayan L, Legido-Quigley C (2008) Advances in separation science applied to metabolomics. *Electrophoresis* 29(18):3724–3736
39. Smolinska A, Blanchet L, Buydens LM, Wijmenga SS (2012) NMR and pattern recognition methods in metabolomics: from data acquisition to biomarker discovery: a review. *Anal Chim Acta* 750:82–97
40. Barding GA, Salditos R, Larive CK (2012) Quantitative NMR for bioanalysis and metabolomics. *Anal Bioanal Chem* 404(4):1165–1179
41. Putri SP, Yamamoto S, Tsugawa H, Fukusaki E (2013) Current metabolomics: technological advances. *J Biosci Bioeng* 116(1):9–16
42. Barbas C, Moraes EP, Villaseñor A (2011) Capillary electrophoresis as a metabolomics tool for non-targeted fingerprinting of biological samples. *J Pharm Biomed Anal* 55(4):823–831
43. Rojo D, Barbas C, Rupérez FJ (2012) LC-MS metabolomics of polar compounds. *Bioanalysis* 4(10):1235–1243
44. Koek MM, Jellema RH, van der Greef J, Tas AC, Hankemeier T (2011) Quantitative metabolomics based on gas chromatography mass spectrometry: status and perspectives. *Metabolomics* 7(3):307–328
45. Creek DJ, Jankevics A, Breitling R, Watson DG, Barrett MP, Burgess KE (2011) Toward global metabolomics analysis with hydrophilic interaction liquid chromatography-mass spectrometry: improved metabolite identification by retention time prediction. *Anal Chem* 83(22):8703–8710
46. Requena JM (2011) Lights and shadows on gene organization and regulation of gene expression in *Leishmania*. *Front Biosci (Landmark Ed)* 16:2069–2085
47. Chawla B, Jhingran A, Panigrahi A, Stuart KD, Madhubala R (2011) Paromomycin affects translation and vesicle-mediated trafficking as revealed by proteomics of paromomycin -susceptible -resistant *Leishmania donovani*. *PLoS One* 6(10):e26660
48. Paape D, Aebischer T (2011) Contribution of proteomics of *Leishmania spp.* to the understanding of differentiation, drug resistance mechanisms, vaccine and drug development. *J Proteomics* 74(9):1614–1624
49. Vergnes B, Gourbal B, Girard I, Sundar S, Drummelsmith J, Ouellette M (2007) A proteomics screen implicates HSP83 and a small kinetoplastid calpain-related protein in drug resistance in *Leishmania donovani* clinical field isolates by modulating drug-induced programmed cell death. *Mol Cell Proteomics* 6(1):88–101
50. Doyle MA, MacRae JI, De Souza DP, Saunders EC, McConville MJ, Likić VA (2009) LeishCyc: a biochemical pathways database for *Leishmania major*. *BMC Syst Biol* 3:57
51. Creek DJ, Anderson J, McConville MJ, Barrett MP (2012) Metabolomic analysis of trypanosomatid protozoa. *Mol Biochem Parasitol* 181(2):73–84
52. McConville MJ, Naderer T (2011) Metabolic pathways required for the intracellular survival of *Leishmania*. *Annu Rev Microbiol* 65:543–561
53. Opperdoes FR, Coombs GH (2007) Metabolism of *Leishmania*: proven and predicted. *Trends Parasitol* 23(4):149–158
54. Scheltema RA, Decuyper S, T'kindt R, Dujardin JC, Coombs GH, Breitling R (2010) The potential of metabolomics for *Leishmania* research in the post-genomics era. *Parasitology* 137(9):1291–1302
55. Lamour SD, Choi BS, Keun HC, Müller I, Saric J (2012) Metabolic characterization of *Leishmania major* infection in activated and non-activated macrophages. *J Proteome Res* 11(8):4211–4222
56. Canuto GA, Castilho-Martins EA, Tavares M, López-González A, Rivas L, Barbas C (2012) CE-ESI-MS metabolic fingerprinting of *Leishmania* resistance to antimony treatment. *Electrophoresis* 33(12):1901–1910
57. T'Kindt R, Scheltema RA, Jankevics A, Brunker K, Rijal S, Dujardin JC, Breitling R, Watson DG, Coombs GH, Decuyper S (2010) Metabolomics to unveil and understand phenotypic diversity between pathogen populations. *PLoS Negl Trop Dis* 4(11):e904
58. Seifert K, Matu S, Javier Pérez-Victoria F, Castanys S, Gamarro F, Croft SL (2003) Characterisation of *Leishmania donovani* promastigotes resistant to hexadecylphosphocholine (miltefosine). *Int J Antimicrob Agents* 22(4):380–387
59. Suhre K, Schmitt-Kopplin P (2008) MassTRIX: mass translator into pathways. *Nucleic Acids Res* 36 (Web Server issue):W481–484.
60. Jiménez-López JM, Rios-Marco P, Marco C, Segovia JL, Carrasco MP (2010) Alterations in the homeostasis of phospholipids and cholesterol by antitumor alkylphospholipids. *Lipids Health Dis* 9:33
61. Verma NK, Dey CS (2004) Possible mechanism of miltefosine-mediated death of *Leishmania donovani*. *Antimicrob Agents Chemother* 48(8):3010–3015
62. Rakotomanga M, Blanc S, Gaudin K, Chaminade P, Loiseau PM (2007) Miltefosine affects lipid metabolism in *Leishmania donovani* promastigotes. *Antimicrob Agents Chemother* 51(4):1425–1430
63. Ramos RG, Libong D, Rakotomanga M, Gaudin K, Loiseau PM, Chaminade P (2008) Comparison between charged aerosol detection and light scattering detection for the analysis of *Leishmania* membrane phospholipids. *J Chromatogr A* 1209(1–2):88–94
64. Geilen CC, Wieder T, Orfanos CE (1996) Phosphatidylcholine biosynthesis as a target for phospholipid analogues. *Adv Exp Med Biol* 416:333–336
65. Seifert K, Pérez-Victoria FJ, Stettler M, Sánchez-Cañete MP, Castanys S, Gamarro F, Croft SL (2007) Inactivation of the miltefosine transporter, LdMT, causes miltefosine resistance that is conferred to the amastigote stage of *Leishmania donovani* and persists in vivo. *Int J Antimicrob Agents* 30(3):229–235
66. T'Kindt R, Jankevics A, Scheltema RA, Zheng L, Watson DG, Dujardin JC, Breitling R, Coombs GH, Decuyper S (2010) Towards an unbiased metabolic profiling of protozoan parasites: optimisation of a *Leishmania* sampling protocol for HILIC-orbitrap analysis. *Anal Bioanal Chem* 398(5):2059–2069
67. Krauth-Siegel RL, Bauer H, Schirmer RH (2005) Dithiol proteins as guardians of the intracellular redox milieu in parasites: old and new drug targets in trypanosomes and malaria-causing plasmodia. *Angew Chem Int Ed Engl* 44(5):690–715
68. Fyfe PK, Westrop GD, Silva AM, Coombs GH, Hunter WN (2012) *Leishmania* TDR1 structure, a unique trimeric glutathione transferase capable of deglutathionylation and antimonial prodrug activation. *Proc Natl Acad Sci U S A* 109(29):11693–11698
69. Wyllie S, Cunningham ML, Fairlamb AH (2004) Dual action of antimonial drugs on thiol redox metabolism in the human pathogen *Leishmania donovani*. *J Biol Chem* 279(38):39925–39932
70. Darlyuk I, Goldman A, Roberts SC, Ullman B, Rentsch D, Zilberstein D (2009) Arginine homeostasis and transport in the human pathogen *Leishmania donovani*. *J Biol Chem* 284(30):19800–19807
71. Castilho-Martins EA, Laranjeira da Silva MF, dos Santos MG, Muxel SM, Floeter-Winter LM (2011) Axenic *Leishmania amazonensis* promastigotes sense both the external and internal arginine pool distinctly regulating the two transporter-coding genes. *PLoS One* 6(11):e27818
72. Basu NK, Kole L, Ghosh A, Das PK (1997) Isolation of a nitric oxide synthase from the protozoan parasite, *Leishmania donovani*. *FEMS Microbiol Lett* 156(1):43–47
73. Genestra M, de Souza WJ, Cysne-Finkelstein L, Leon LL (2003) Comparative analysis of the nitric oxide production by *Leishmania sp.* *Med Microbiol Immunol* 192(4):217–223

74. Saunders EC, Ng WW, Chambers JM, Ng M, Naderer T, Krömer JO, Likic VA, McConville MJ (2011) Isotopomer profiling of *Leishmania mexicana* promastigotes reveals important roles for succinate fermentation and aspartate uptake in tricarboxylic acid cycle (TCA) anaplerosis, glutamate synthesis, and growth. *J Biol Chem* 286(31):27706–27717
75. Inbar E, Canepa GE, Carrillo C, Glaser F, Suter Grotemeyer M, Rentsch D, Zilberstein D, Pereira CA (2012) Lysine transporters in human trypanosomatid pathogens. *Amino Acids* 42(1):347–360
76. Simon MW, Mukkada AJ (1977) *Leishmania tropica*: regulation and specificity of the methionine transport system in promastigotes. *Exp Parasitol* 42(1):97–105
77. Paes LS, Galvez Rojas RL, Daliry A, Floeter-Winter LM, Ramirez MI, Silber AM (2008) Active transport of glutamate in *Leishmania (Leishmania) amazonensis*. *J Eukaryot Microbiol* 55(5):382–387
78. Michels PA, Bringaud F, Herman M, Hannaert V (2006) Metabolic functions of glycosomes in trypanosomatids. *Biochim Biophys Acta* 1763(12):1463–1477
79. Ginger ML, Chance ML, Sadler IH, Goad LJ (2001) The biosynthetic incorporation of the intact leucine skeleton into sterol by the trypanosomatid *Leishmania mexicana*. *J Biol Chem* 276(15):11674–11682
80. Alloatti A, Uttaro AD (2011) Highly specific methyl-end fatty-acid desaturases of trypanosomatids. *Mol Biochem Parasitol* 175(2):126–132
81. Inbar E, Schlisselberg D, Suter Grotemeyer M, Rentsch D, Zilberstein D (2013) A versatile proline/alanine transporter in the unicellular pathogen *Leishmania donovani* regulates amino acid homeostasis and osmotic stress responses. *Biochem J* 449(2):555–566
82. Weingärtner A, Drobot B, Herrmann A, Sánchez-Cañete MP, Gamarro F, Castanys S, Günther Pomorski T (2010) Disruption of the lipid-transporting LdMT-LdRos3 complex in *Leishmania donovani* affects membrane lipid asymmetry but not host cell invasion. *PLoS One* 5(8):e12443
83. Naderer T, McConville MJ (2011) Intracellular growth and pathogenesis of *Leishmania* parasites. *Essays Biochem* 51:81–95
84. Haas A (2007) The phagosome: compartment with a license to kill. *Traffic* 8(4):311–330
85. Verma S, Mehta A, Shaha C (2011) CYP5122A1, a novel cytochrome P450 is essential for survival of *Leishmania donovani*. *PLoS One* 6(9):e25273
86. Reguera RM, Balaña-Fouce R, Showalter M, Hickerson S, Beverley SM (2009) *Leishmania major* lacking arginase (ARG) are auxotrophic for polyamines but retain infectivity to susceptible BALB/c mice. *Mol Biochem Parasitol* 165(1):48–56
87. Rosenzweig D, Smith D, Opperdoes F, Stern S, Olafson RW, Zilberstein D (2008) Retooling *Leishmania* metabolism: from sand fly gut to human macrophage. *FASEB J* 22(2):590–602
88. Saunders EC, DE Souza DP, Naderer T, Sernee MF, Ralton JE, Doyle MA, Macrae JI, Chambers JL, Heng J, Nahid A, Likic VA, McConville MJ (2010) Central carbon metabolism of *Leishmania* parasites. *Parasitology* 137(9):1303–1313
89. Chen M, Zhai L, Christensen SB, Theander TG, Kharazmi A (2001) Inhibition of fumarate reductase in *Leishmania major* and *L. donovani* by chalcones. *Antimicrob Agents Chemother* 45(7):2023–2029
90. Carvalho L, Luque-Ortega JR, López-Martín C, Castanys S, Rivas L, Gamarro F (2011) The 8-aminoquinoline analogue sitamaquine causes oxidative stress in *Leishmania donovani* promastigotes by targeting succinate dehydrogenase. *Antimicrob Agents Chemother* 55(9):4204–4421